ISSN: 2634-9221
European Journal of Applied Sciences; Vol. 14 No. 02 (2026) (567-576)
https://doi.org/10.14738/aivp.1402.20237

# Non-Hermitian Dynamics and Decoherence of Bell States in a Bosonic Dissipative System

Lin Xiao and Qing-Xu Li*

1. School of Electronic Science and Engineering, Chongqing University of Posts and Telecommunications, Chongqing 400065, China

**Abstract:** We theoretically investigate the state evolution and decoherence of Bell states in a two-qubit system coupled to local bosonic thermal baths. By employing a hybrid Liouvillian formalism with a tuning parameter $q$, we systematically explore the transition from purely non-Hermitian coherent evolution ($q = 0$) to complete Lindblad master equation dynamics ($q = 1$) in a bosonic environment. Our results demonstrate that at $q = 0$, dynamically encircling a second-order exceptional point (EP) enables a near-perfect chiral transfer between the Bell states $|\Phi^+\rangle$and $|\Phi^-\rangle$. This phenomenon is shown to be globally robust against variations in the bosonic thermal occupation numbers of the environment. However, the introduction of quantum jump processes ($q > 0$) significantly suppresses the directional selectivity, and the chirality completely disappears in the full Liouvillian limit ($q = 1$). Furthermore, we find that the dissipative protocol is unable to generate entanglement starting from a maximally mixed state, highlighting the role of initial state purity. This work elucidates the interplay between non-Hermitian topology and bosonic decoherence, providing insights for state evolution in realistic open quantum systems.

## INTRODUCTION

The study of open quantum systems has been profoundly enriched by the advent of non-Hermitian physics, which provides a powerful framework for describing dissipation and continuous energy exchange with a reservoir. A hallmark of non-Hermitian systems is the existence of exceptional points (EPs), degenerate singularities where both eigenvalues and their corresponding eigenvectors coalesce. Unlike conventional Hermitian degeneracies, EPs possess non-trivial topological properties, often characterized by the winding of Riemann surfaces in their complex energy spectra. These unique topological features have spurred extensive theoretical and experimental efforts, leading to the discovery of novel physical phenomena such as enhanced quantum sensing, unidirectional invisibility, and topological mode switching.

In real-world quantum architectures, systems are inevitably coupled to bosonic environments, such as electromagnetic fields or lattice vibrations, which lead to intrinsic dissipation and decoherence. One of the most striking consequences of EP topology in such environments is the chiral state transfer. When the system parameters are adiabatically modulated to encircle an EP in the parameter space [1, 2], the system's final state is determined entirely by the direction of the encirclement, largely independent of the initial state. However, theoretical descriptions often rely on effective non-Hermitian Hamiltonians, assuming a post-selection process where no quantum jumps occur [3]. In

* liqx@cqupt.edu.cn

realistic bosonic dissipative systems, a complete physical description requires the Lindblad master equation, which incorporates the full dynamics including stochastic quantum jumps. The presence of these jumps can inherently disrupt the coherent non-Hermitian evolution, raising critical questions about the robustness of such topological state transfers against environmental bosonic noise.

Motivated by this, we investigate the non-Hermitian dynamics and decoherence of Bell states in a two-qubit system coupled to local bosonic thermal baths. By employing a hybrid Liouvillian formalism with a tuning parameter $q$ [4], we seamlessly bridge the purely nonHermitian coherent evolution ($q = 0$) and the complete Lindblad master equation dynamics ($q = 1$). We demonstrate that while the chiral transfer is remarkably robust against bosonic thermal fluctuations at $q = 0$, it is highly sensitive to the inclusion of quantum jumps. Furthermore, we reveal that this dissipative protocol cannot generate entanglement from a maximally mixed initial state. These findings provide profound insights into the interplay between non-Hermitian topology and bosonic decoherence, establishing a theoretical foundation for understanding state evolution in practical open quantum systems.

## MODEL

We consider a system consisting of two qubits with respective energy gaps $\epsilon_1$ and $\epsilon_2$. The energy detuning between the two qubits is defined as $\Delta\epsilon = \epsilon_2 - \epsilon_1$. The two qubits are mutually coupled with an interaction strength $g$, and each qubit is individually coupled to a local bosonic thermal bath at temperature $T_j$ (where $j = 1,2$) with a system-bath coupling strength $\gamma_j$, as schematically shown in Fig. 1. The total Hamiltonian of the system can be written as:

$$H = H_s + H_{\text{int}} + H_{\text{B}} + H_{\text{SB}}, \tag{1}$$

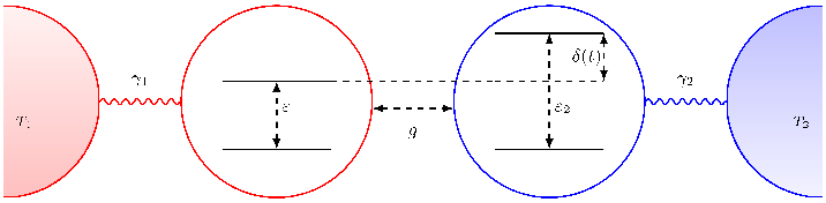


**Fig. 1: Schematic diagram of the coupled two-qubit model with local bosonic thermal baths.**

where $H_s$ is the Hamiltonian of the two-level system, $H_{\text{int}}$ is their interaction Hamiltonian, $H_{\text{B}}$ is the Hamiltonian of the two bosonic baths, and $H_{\text{SB}}$ is the systembath interaction Hamiltonian. Their specific forms are:

$$\begin{aligned} H_s &= \tfrac{\epsilon_1+\epsilon_2}{2} I + \tfrac{\epsilon_1}{2}\sigma_1^z - \tfrac{\epsilon_2}{2}\sigma_2^z \\ H_{\text{int}} &= g(\sigma_1^+\sigma_2^- + \sigma_1^-\sigma_2^+) \\ H_{\text{B}} &= \textstyle\sum_{j\in\{1,2\}} \omega_j b_j^\dagger b_j \\ H_{\text{SB}} &= \textstyle\sum_{j\in\{1,2\}} \left(a_j\sigma_j^- b_j^\dagger + a_j^*\sigma_j^+ b_j\right) \end{aligned} \tag{2}$$

Here, $\sigma^z$ is the Pauli- $z$ operator, and $\sigma_j^+$and $\sigma_j^-$ represent the raising and lowering operators for the $j$-th qubit, respectively. Since the excited state of qubit 1 is $|0\rangle_1$, we have $\sigma_1^+ = |0\rangle_1\langle 1|_1$, corresponding to an excitation process, and $\sigma_1^- = |1\rangle_1\langle 0|_1$, corresponding to a de-excitation process. For qubit 2, the excited state is $|1\rangle_2$, and correspondingly, $\sigma_2^+ = |1\rangle_2\langle 0|_2$ and $\sigma_2^- =| 0\rangle_2\langle 1|_2$. The singlequbit basis is taken as $|0\rangle := (1,0)^{\mathrm{T}}$ and $|1\rangle := (0,1)^{\mathrm{T}}$ (for $j = 1,2$ ). The bath modes are described by bosonic creation and annihilation operators $b_j^\dagger$ and $b_j$ , with energy $\omega_j$ , satisfying $\left[b_j, b_i^\dagger\right] = \delta_{ij}$ . The coefficient $a_j$ quantifies the interaction strength between the $j$-th qubit and its corresponding bosonic thermal bath.

In the following discussion, we set $\hbar = 1$ and $k_{\mathrm{B}} = 1$. Under the weak-coupling condition $\left(g \lesssim \gamma_j \ll \epsilon_j\right)$, the time evolution of the system can be described by the Lindblad equation [5-7]:

$$\begin{aligned}\frac{\partial\hat{\rho}(t)}{\partial t} = \mathcal{L}\hat{\rho}(t) = &-i\left[\hat{H}_{\mathrm{eff}}\hat{\rho}(t) - \hat{\rho}(t)\hat{H}_{\mathrm{eff}}^\dagger\right] \\ &+ \textstyle\sum_{j=1,2}\left(\gamma_j^+\mathcal{D}_+^{(j)}\rho(t) + \gamma_j^-\mathcal{D}_-^{(j)}\rho(t)\right),\end{aligned} \tag{3}$$

where the effective non-Hermitian Hamiltonian (NHH) of the system can be expressed as

$$H_{\mathrm{eff}} = H_s + H_{\mathrm{int}} - \frac{i}{2}\textstyle\sum_{j=1}^{2}\left(\gamma_j^+\sigma_j^-\sigma_j^+ + \gamma_j^-\sigma_j^+\sigma_j^-\right), \tag{4}$$

which consists of the unitary evolution part of the system $H_s + H_{\mathrm{int}}$ and the coherent dissipation induced by the bosonic environment. Here, $\gamma_j^+$and $\gamma_j^-$represent the incoming and outgoing rates of qubit $j$, respectively. Under the bosonic bath approximation, they take the form

$$\gamma_j^+(\varepsilon_j) = \gamma_j n_j(\varepsilon_j), \gamma_j^-(\varepsilon_j) = \gamma_j\left(1 + n_j(\varepsilon_j)\right), \tag{5}$$

where $\gamma_j(E) = 2\pi\left|\alpha_j\right|^2\delta(E - \varepsilon_j)$, and

$$n_j = \left(e^{\beta_j(\epsilon_1+\epsilon_2)/2} - 1\right)^{-1} \tag{6}$$

is the Bose-Einstein distribution function, with $\beta_j = 1/T_j$ being the inverse temperature of the $j$-th bosonic thermal bath. Furthermore, the dissipative superoperator $\mathcal{D}_\pm^{(j)}\rho := \sigma_\pm^{(j)}\rho\sigma_\mp^{(j)}$ describes the quantum jump processes arising from continuous measurement by the bosonic thermal baths, whose physical origin stems from the persistent monitoring of the system by the environment [8-10].

By invoking a continuous measurement protocol with post-selection, we can introduce a hybrid Liouvillian equation with a tuning parameter $q \in [0,1]$ : when $q = 0$, the equation reduces to the evolution dominated solely by the effective non-Hermitian Hamiltonian; when $q = 1$, it recovers the Lindblad master equation that includes the full quantum jump terms. By continuously varying the parameter $q$, one can systematically trace the transition of the system from purely non-Hermitian coherent evolution to the complete quantum master equation evolution [4]. The explicit form of this equation is as follows:

$$\begin{aligned}\frac{\partial\hat{\rho}(t)}{\partial t} = \mathcal{L}_q\hat{\rho}(t) = &-i\left[\hat{H}_{\mathrm{eff}}\hat{\rho}(t) - \hat{\rho}(t)\hat{H}_{\mathrm{eff}}^\dagger\right] \\ &+ q\textstyle\sum_{j=1,2}\left(\gamma_j^+\mathcal{D}_+^{(j)}\rho(t) + \gamma_j^-\mathcal{D}_-^{(j)}\rho(t)\right),\end{aligned} \tag{7}$$

where $\mathcal{L}_q$ is the Liouville superoperator that depends on the parameter $q$.

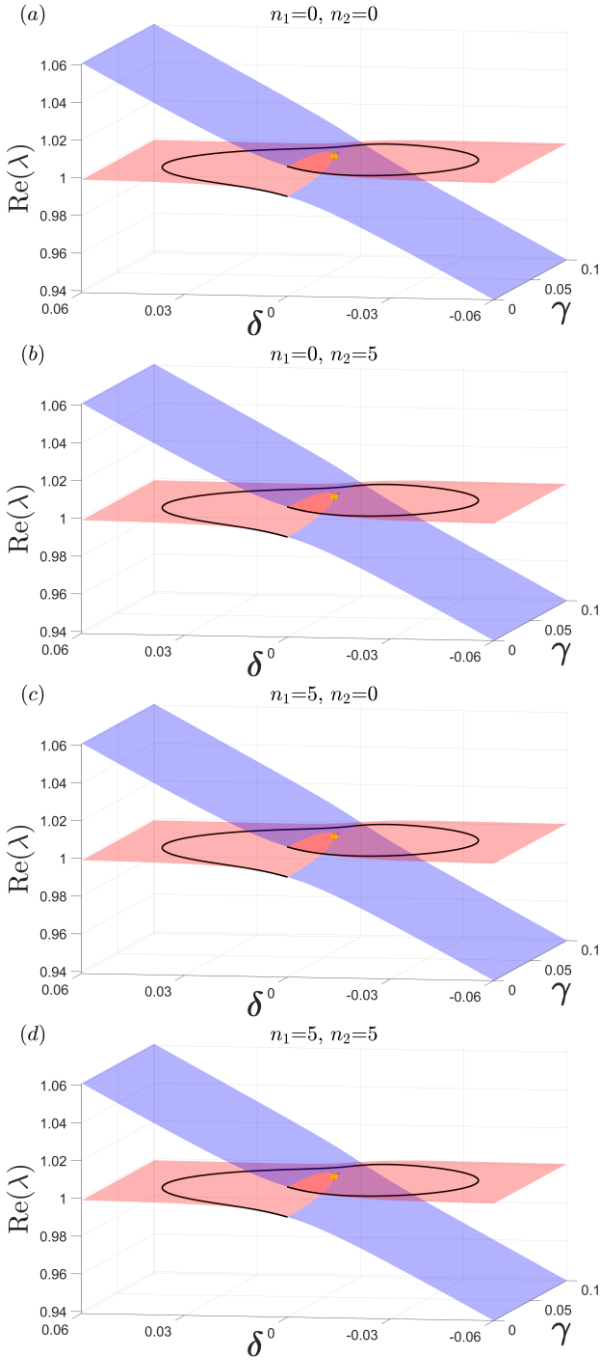


**Fig. 2: The Riemann sheets corresponding to the eigenvalues of the effective non-Hermitian Hamiltonian. The branch with stronger decay (i.e., the branch with a more negative imaginary part) is drawn in red. The yellow point marks the exceptional point (EP) of the Liouvillian operator at $q = 0$**

The effective non-Hermitian Hamiltonian exhibits a second-order exceptional point (EP) when the parameters satisfy $\delta = 0$ and $4g = \gamma_1^+ - \gamma_1^- - \gamma_2^+ + \gamma_2^-$. Performing adiabatic evolution along a closed path near the EP is a key condition for achieving chiral state transfer: the direction of encircling (clockwise or counterclockwise) determines the specific behavior of the state exchange, and its physical mechanism is closely related to the

topological structure of the Riemann surface associated with the eigenvalues of $H_{\text{eff}}$ [11, 12]. Figure 2 shows the Riemann surfaces of the real parts of the Hamiltonian eigenvalues in the parameter space ( $\delta,\gamma$ ), where the red branch corresponds to the eigenstate with stronger decay (i.e., more negative imaginary part). We plot these Riemann surfaces for four different combinations of bosonic thermal occupations: $(n_1 = 0, n_2 = 0)$, $(n_1 = 0, n_2 = 5)$, ( $n_1 = 5, n_2 = 0$ ), and ( $n_1 = 5, n_2 = 5$ ). The results indicate that in all four cases, the Riemann surfaces exhibit topologically non-trivial sheet structures. As shown in Fig. 2, although the parameter values differ, the positions of the branch points and the connection patterns of the Riemann sheets do not undergo exchange or fundamental changes, indicating the stability of their topological structure. Consequently, the directional selection rule for chiral state transfer should remain consistent across different parameter settings.

To discuss the chiral behavior of state transfer near the exceptional point (EP) in the parameter space $(\delta,\gamma)$, we set $\gamma_1 = \gamma, \gamma_2 = \alpha\gamma$, and consider the coupling strength $\gamma$ and detuning $\delta$ as time-periodically modulated parameters. The driving forms are chosen as:

$$\begin{aligned}\gamma(t) &= \gamma_0 + \Delta\gamma \sin^2\left(\frac{\pi t}{T}\right)\\ \delta(t) &= \pm\Delta\delta \sin\left(\frac{2\pi t}{T}\right)\end{aligned} \tag{8}$$

where $T$ is the driving period, $\gamma_0$ is the offset, and $\Delta\gamma$ and $\Delta\delta$ are the amplitudes of $\gamma(t)$ and $\delta(t)$, respectively. The "+" and "-" signs in the expression for $\delta(t)$ correspond to closed paths evolving in the clockwise and counterclockwise directions in the parameter space, respectively. As shown in Fig. 2, this path forms a closed trajectory (black curve) on the $(\gamma,\delta)$ plane. By appropriately choosing $\Delta\gamma$, this trajectory can be made to encircle the exceptional point (EP).

## CHIRAL BELL-STATE TRANSFER

Given that the initial state of the system is $\rho(0)$, the unnormalized density matrix at time $t$ can be expressed as:

$$\rho(t) = \mathcal{T}\exp\left[\int_0^t \mathcal{L}_q(t')dt'\right]\rho(0) \tag{9}$$

where $\mathcal{T}$ denotes the time-ordering operator, and $\mathcal{L}_q$ is the superoperator that governs the dynamics. It is important to note that when $0 \le q < 1$, this dynamical process does not preserve trace conservation. When $\delta = \gamma = 0$ (i.e., at $t = 0$ and $t = T$ ), the effective nonHermitian Hamiltonian $H_{\text{eff}}$ reduces to the total system Hamiltonian $H_s + H_{\text{int}}$ . At this point, the eigenstate set of $H_s + H_{\text{int}}$ is given by $\left\{|10\rangle, |\Phi^+\rangle = \frac{|11\rangle+|00\rangle}{\sqrt{2}}, |\Phi^-\rangle = \frac{|11\rangle-|00\rangle}{\sqrt{2}}, |01\rangle\right\}$. Consequ-ently, the Liouville superoperator simplifies to the form governing standard unitary evolution:

$$\mathcal{L}\hat{\rho}(t) = -i\left[\left(\hat{H}_s + \hat{H}_{\text{int}}\right)\hat{\rho}(t) - \hat{\rho}(t)\left(\hat{H}_s + \hat{H}_{\text{int}}\right)^{\dagger}\right]. \tag{10}$$

Under this specific condition, the eigenvectors of $\mathcal{L}$ can be directly constructed from the eigenvectors of $H_s + H_{\text{int}}$ . This property serves as the key mechanism enabling chiral state transfer. To quantitatively characterize the degree of proximity between the system's state and the target Bell state during evolution, we define the fidelity of the even-parity Bell states $|\Phi^{\pm}\rangle$as:

$$\mathcal{F}_{|\Phi^{\pm}\rangle}(t) := \mathrm{Tr}\left[|\Phi^{\pm}\rangle\langle\Phi^{\pm}|\rho(t)\right]. \tag{11}$$

Figure 3 shows the time evolution of the fidelity $\mathcal{F}_{|\Phi^-\rangle}(t)$ for the target state $|\Phi^-\rangle$ with $|\Phi^+\rangle$ as the initial state, under different thermal occupation combinations $(n_1, n_2) = (0,0), (0,5), (5,0)$, and $(5,5)$.

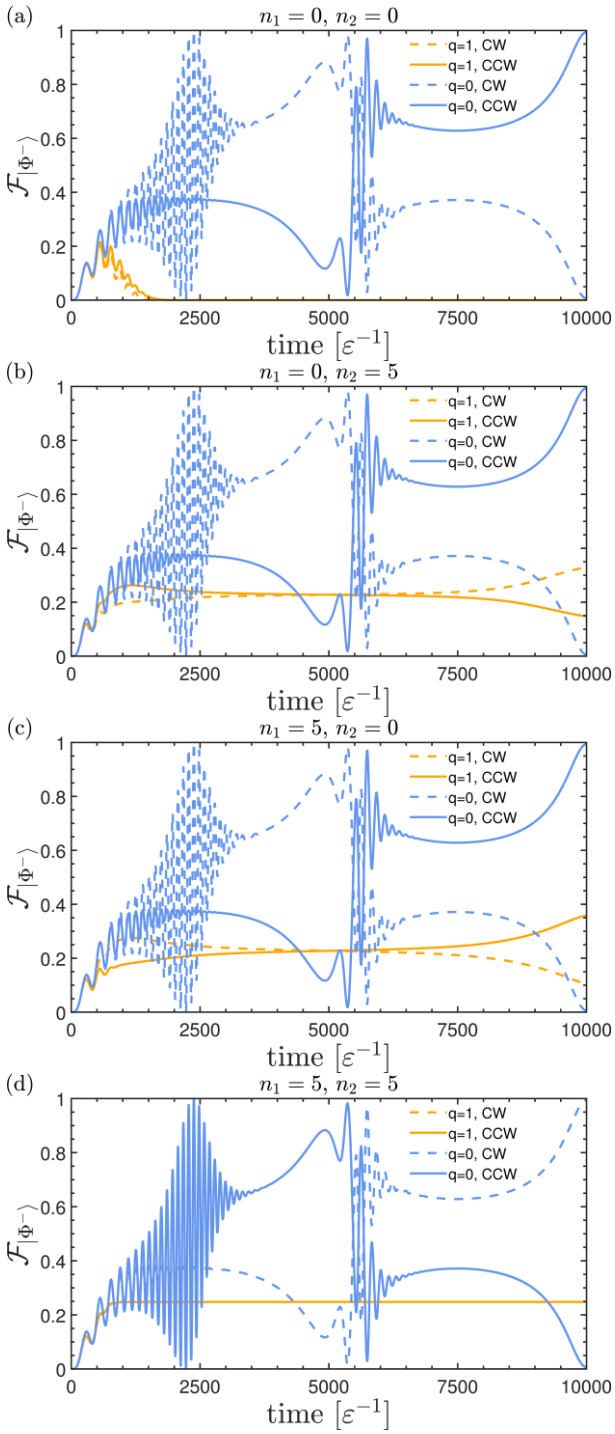


**Fig. 3: Evolution of the fidelity of the even-parity Bell states $|\Phi^-\rangle$over time (dashed lines for clockwise trajectories, solid lines for counterclockwise trajectories). The parameters are $\varepsilon = 1, \alpha = 0.5, g/\varepsilon = 0.008, \Delta\delta/\varepsilon = 0.06, \Delta\gamma = 0.03, \gamma_0 = 0$, and $T\varepsilon = 10000$.**

When $q = 0$, panels (a)-(d) demonstrate the following: when the system evolves along the clockwise (CW) path to $t = T$, the fidelity $\mathcal{F}_{|\Phi^-\rangle}(T) \approx 1$, indicating successful transfer to the target state $|\Phi^-\rangle$. Conversely, when evolving along the counterclockwise (CCW) path, the fidelity $\mathcal{F}_{|\Phi^-\rangle}(T) \approx 0$, meaning the system largely remains in the initial state $|\Phi^+\rangle$. This reveals that clear chiral state transfer occurs under all four thermal occupation combinations at $q = 0$, and this phenomenon is robust against variations in thermal occupations.

When $q = 1$, the chiral transfer behavior disappears. Specifically: for $(n_1, n_2) = (0,0)$, the final-state fidelities for both CW and CCW paths are 0 ; for $(5,5)$, both are approximately 0.247 ; for ( 0,5 ), the CW-path fidelity is about 0.379 , while the CCW-path fidelity is about 0.079 ; and for $(5,0)$, the CW-path fidelity is about 0.148 , while the CCW-path fidelity is about 0.328 . None of these results exhibit the clear chiral selectivity observed at $q = 0$ .

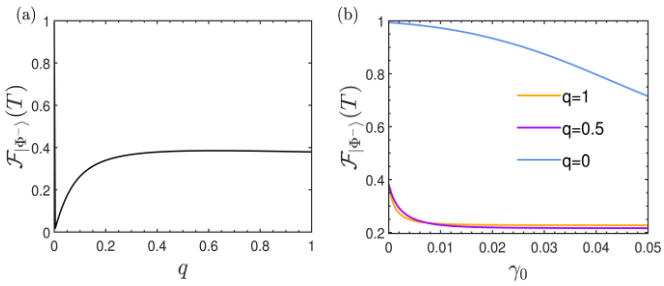


**Fig. 4: Evolution of the final fidelity $\mathcal{F}_{|\Phi^-\rangle}(T)$ as a function of (a) the quantum jump parameter $q$ and (b) the parameter $\gamma_0$, for the clockwise evolution path. Parameters: $n_1 = 0, n_2 = 5$, other parameter values are consistent with those in Fig. 3.**

To systematically investigate the influence of the quantum, jump parameter $q$, Fig. 4(a) presents the variation of the final-state fidelity $\mathcal{F}_{|\Phi^-\rangle}(T)$ with respect to $q$ along the clockwise (CW) path for $(n_1, n_2) = (0,5)$. It can be observed that when $q = 0$, the fidelity is close to 1 . Once $q \neq 0$, the fidelity drops sharply to approximately 0.01. Subsequently, as $q$ increases, the fidelity gradually recovers, reaches a plateau around 0.38 , and no longer changes with further increases in $q$.

Furthermore, Fig. 4(b) shows curves of $\mathcal{F}_{|\Phi^-\rangle}(T)$ as a function of the dissipation strength $\gamma_0$ for different values of $q$. The results indicate that regardless of the value of $q$, the fidelity decreases as $\gamma_0$ increases. In particular, for the case of $q = 0$, a non-zero $\gamma_0$ causes the even-parity Bell states $|\Phi^{\pm}\rangle$to no longer be eigenstates of the nonHermitian Hamiltonian at the starting and ending points of the evolution trajectory. This breaks the adiabatic eigenpath essential for chiral state transfer, which is the physical origin of the fidelity reduction in this scenario.

We now analyze the dependence of the final-state fidelity $\mathcal{F}_{|\Phi^-\rangle}(T)$ on the thermal occupation numbers $n_1$ and $n_2$ for the two cases of $q = 0$ and $q = 1$.

From Fig. 5(a) and (c), it can be observed that when $q = 0$, the final-state fidelity along the clockwise (CW) path remains close to 1 across the entire parameter range of $(n_1, n_2)$ , independent of the values of $n_j$ . Correspondingly, the fidelity along the counterclockwise (CCW) path remains close to 0 . This indicates that at $q = 0$, the system

undergoes nearly perfect chiral state transfer along the CW path, and this phenomenon exhibits global robustness against variations in thermal occupations. This behavior originates from the eigenstructure of the effective non-Hermitian Hamiltonian: as shown in Fig. 2, the Riemann surfaces maintain the same topological structure for different $(n_1, n_2)$ values, without phenomena such as level inversion or movement of degeneracy points. Consequently, the direction of chiral evolution does not change with variations in thermal occupation numbers.

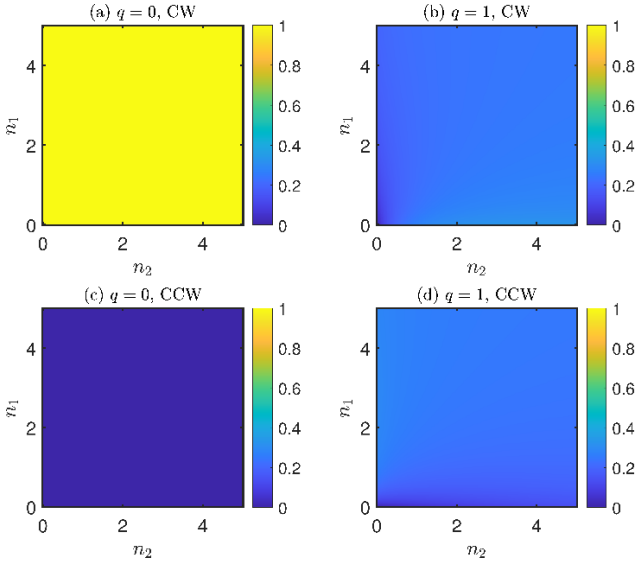


**Fig. 5: Dependence of the final fidelity $\mathcal{F}_{|\Phi^-\rangle}(T)$ on the thermal occupation numbers $n_1$ and $n_2$ along the clockwise evolution path. All other parameter settings are the same as in Fig. 3.**

When $q = 1$, the situation is entirely different. Fig. 5(b) and (d) reveal that, regardless of whether the evolution follows the CW or CCW path, the final-state fidelity remains around 0.2 , and the fidelity distributions for the two paths show no significant difference, exhibiting no directional selectivity. This indicates that under full Liouvillian dynamics (i.e., the evolution of the system without post-selection), the phenomenon of chiral state transfer disappears.

In summary, only in the limit of complete postselection corresponding to $q = 0$, where the system is governed by the effective non-Hermitian Hamiltonian, can clear and thermally robust chiral state transfer be achieved. Once quantum jump processes are introduced $(q \neq 0)$, this chiral characteristic is destroyed.

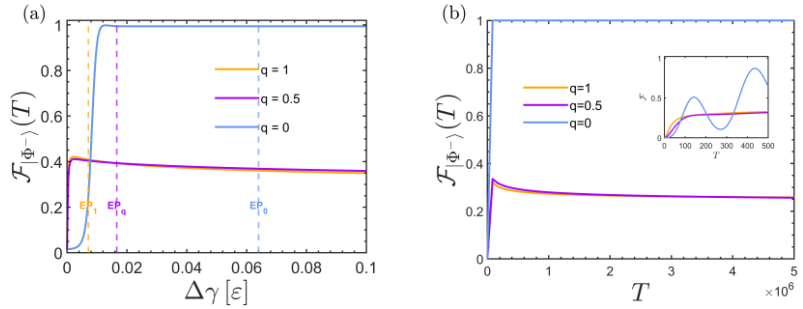


**Fig. 6: Dependence of the final-state fidelity $F_{|\Phi^+\rangle}$on the path amplitude $\Delta\gamma$ and the driving period $T$**

Fig. 6(a) shows the dependence of the final-state fidelity on the path amplitude $\Delta\gamma$. The vertical dashed line indicates the position of the exceptional point (EP) of the Liouvillian operator: the left side of the line corresponds to a parameter trajectory that does not encircle the EP, while the right side corresponds to one that does. It can be observed that regardless of the value of $q$, the fidelity curves show no significant abrupt changes across the EP, indicating that under this parameter setting, whether or not the EP is encircled has a negligible effect on the final-state fidelity. Fig. 6(b) presents the variation of the final-state fidelity with the driving period $T$. The results show that when $T$ is sufficiently large, the final-state fidelity for different values of $q$ stabilizes and no longer varies with $T$. Of particular note is that in the case of $q = 0$, by choosing a sufficiently slow driving period (i.e., satisfying the adiabatic condition), the system can achieve nearly perfect chiral state transfer with fidelity approaching 1 .

## STATE EVOLUTION FROM THE MAXIMALLY MIXED STATE

Next, we explore the state evolution starting from a maximally separable initial state. The system starts from the maximally mixed state $\rho(0) = I/4$ under periodic parameter driving. To quantify entanglement, we introduce the concurrence [13]:

$$\mathcal{C}(\rho) := 2\max\{0, |d| - \sqrt{p_{01}p_{10}}\} \tag{12}$$

where $p_{01} = \langle 01|\rho|01\rangle$, $p_{10} = \langle 10|\rho|10\rangle$, and the offdiagonal element $d = \langle 00|\rho|11\rangle$ reflects the coherence between the $|00\rangle$ and $|11\rangle$ levels. Under this measure, $\mathcal{C} = 0$ corresponds to a separable state, while $\mathcal{C} = 1$ corresponds to a maximally entangled state.

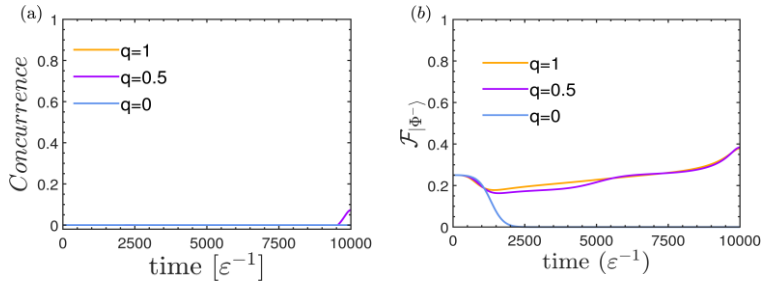


**Fig 7: Evolution of (a) concurrence $C(t)$ and (b) fidelity $\mathcal{F}_{|\Phi^-\rangle}(t)$ over time $t$, starting from the initial state $\rho(0) = I/4$. All parameter settings are the same as in Fig. 4.**

Fig. 7(a) shows the time evolution of the concurrence. The results indicate that for different values of $q$, the concurrence remains close to zero, suggesting that under this initial condition, entangled states cannot be effectively generated from the maximally separable state in such a bosonic dissipative system. This conclusion is further supported by Fig. 7(b), which displays the evolution of the fidelity $\mathcal{F}_{|\Phi^-\rangle}(t)$ of the target state $|\Phi^-\rangle$. It can be seen that the system remains far from this even-parity Bell state throughout the entire evolution.

## CONCLUSION

In conclusion, we have investigated the state evolution of a two-qubit system coupled to local bosonic thermal baths using a hybrid Liouvillian approach. Our analysis reveals that

perfect chiral state transfer is achievable in the post-selection limit ($q = 0$), where the dynamics are governed by the effective non-Hermitian Hamiltonian. Notably, this robust evolution is maintained against variations in the bosonic thermal occupations, a property rooted in the stable topological structure of the associated Riemann surfaces. However, the introduction of quantum jumps ($q > 0$) acts as a strong decoherence mechanism that destroys the directional selectivity of the transfer process. We also find that the current protocol is unable to create entangled states from a maximally mixed initial state. These results provide a detailed understanding of how non-Hermitian topological features compete with environmental bosonic noise, offering a theoretical basis for understanding decoherence in realistic open quantum systems.

## REFERENCES


[1] J. Doppler, A. A. Mailybaev, J. Böhm, U. Kuhl, A. Girschik, F. Libisch, T. J. Milburn, P. Rabl, N. Moi- seyev, and S. Rotter, "Dynamically encircling an exceptional point for asymmetric mode switching," Nature, vol. 537, pp. 76–79, 2016.

[2] H. Xu, D. Mason, L. Jiang, and J. G. E. Harris, "Topo- logical energy transfer in an optomechanical system with exceptional points," Nature, vol. 537, pp. 80-83, 2016.

[3] H. J. Carmichael, "Quantum trajectory theory for cascading master equations," Physical Review Letters, vol. 70, p. 2273, 1993.

[4] F. Minganti, A. Miranowicz, R. W. Chhajlany, I. I. Arkhipov, and F. Nori, "Hybrid-Liouvillian formalism connecting exceptional points of non-Hermitian Hamiltonians and Liouvillians via postselection of quantum trajectories," Physical Review A, vol. 101, p. 062112, 2020.

[5] H. M. Wiseman and G. J. Milburn, Quantum Measurement and Control. Cambridge, UK: Cambridge University Press, 2010.

[6] H.-P. Breuer and F. Petruccione, The Theory of Open Quantum Systems. Oxford: Oxford University Press, 2007.

[7] P. P. Hofer, M. Perarnau-Llobet, L. D. M. Miranda, G. Haack, R. Silva, J. B. Brask, and N. Brunner, "Marko- vian master equations for quantum thermal machines: Local versus global approach," New Journal of Physics, vol. 19, p. 123037, 2017.

[8] M. G. A. Paris, "The modern tools of quantum mechanics: A tutorial on quantum states, measurements, and operations," The European Physical Journal Special Topics, vol. 203, pp. 61–86, 2012.

[9] S. Haroche and J.-M. Raimond, Exploring the Quantum: Atoms, Cavities, and Photons. Oxford: Oxford University Press, 2006.

[10] S. M. Barnett, Quantum Information. Oxford: Oxford University Press, 2009.

[11] H. Nasari, G. Lopez-Galmiche, H. E. Lopez-Aviles, A. Schumer, A. U. Hassan, Q. Zhong, S. Rotter, P. LiKamWa, D. N. Christodoulides, and M. Kha- javikhan, "Observation of chiral state transfer with- out encircling an exceptional point," Nature, vol. 605, pp. 256-261, 2022.

[12] W. Chen, M. Abbasi, B. Ha, S. Erdamar, Y. N. Joglekar, and K. W. Murch, "Decoherence-Induced Exceptional Points in a Dissipative Superconducting Qubit," Physical Review Letters, vol. 128, p. 110402, 2022.

[13] W. K. Wootters, "Entanglement of Formation of an Arbitrary State of Two Qubits," Physical Review Letters, vol. 80, pp. 2245-2248, 1998.